Coupling discrete metal nanoparticles to photonic crystal surface resonant modes and application to Raman spectroscopy

Seok-min Kim[1*], Wei Zhang[2], Brian T. Cunningham[3]

[1]*School of Mechanical Engineering, Chung-Ang University, 221 Heukseok-dong, Dongjak-gu, Seoul 156-756, Korea*
[2] *Molecular Imprints Inc. 1807 West Braker Lane, Austin, Texas 78758, USA*
[3]*Department of Electrical and Computer Engineering, University of Illinois at Urbana-Champaign, Micro and Nanotechnology Laboratory, 208 North Wright Street, Urbana, Illinois 61801, USA*
[*]*smkim@cau.ac.kr*

Abstract: Coupling a tightly packed layer of discrete metal nanoparticles to the resonant mode of a photonic crystal surface has been demonstrated as a means for obtaining additional electromagnetic gain for surface-enhanced Raman spectroscopy (SERS), in which electric fields of the photonic crystal can couple to plasmon resonances of the metal nanoparticles. Because metal nanoparticles introduce absorption that quench the photonic crystal resonance, a balance must be achieved between locating the metal nanoparticles too close to the surface while still positioning them within the enhanced evanescent field to maximize coupling to surface plasmons. In this work, we describe a parametric study into the design of a photonic crystal-SERS substrate, comprised of a replica molded photonic crystal slab as the dielectric optical resonator, a SiO_2 "post" layer spacer, and an Ag "cap" metal nanostructure. Using the Raman signal for trans-1,2-bis(4pyridyl)ethane, the coupling efficiency was maximized for a SiO_2 "post" layer thickness of 50 nm and a Ag "cap" height of ~20 nm, providing an additional enhancement factor of 21.4.

OCIS codes: (050.5298) Photonic crystals; (240.6695) Surface enhanced Raman spectroscopy; (240.6680) Surface plasmons; (230.4555) Coupled resonators; (220.4241) Nanostructure fabrication; (280.4788) Optical sensing and sensors

References and links

1. J. M. Reyes-Goddard MSc, H. Barr, and N. Stone, "Photodiagnosis using Raman and surface enhanced Raman scattering of bodily fluids," Photodiagn. Photodyn. Ther. **2**(3), 223–233 (2005).
2. I. Pochrandc, *Springer Tracts in Modern Physics* (Springer-Verlag, 1984).
3. D. A. Weitz, M. Moskovits, and J. A. Creighton, "Surface-enhanced Raman spectroscopy with emphasis on liquid-solid interfaces," in *Chemical Structure at Interfaces:New Laser and Optical Techniques*, R. B. Hall and A.B. Ellis, eds. (VCH, 1986), pp. 197–243.
4. J. A. Dieringer, A. D. McFarland, N. C. Shah, D. A. Stuart, A. V. Whitney, C. R. Yonzon, M. A. Young, X. Zhang, and R. P. Van Duyne, "Surface enhanced Raman spectroscopy: new materials, concepts, characterization tools, and applications," Faraday Discuss. **132**, 9–26 (2006).
5. A. Gopinath, S. V. Boriskina, W. R. Premasiri, L. Ziegler, B. M. Reinhard, and L. Dal Negro, "Plasmonic nanogalaxies: multiscale aperiodic arrays for surface-enhanced Raman sensing," Nano Lett. **9**(11), 3922–3929 (2009).
6. C. Lin, L. Jiang, Y. Chai, H. Xiao, S. Chen, and H. Tsai, "One-step fabrication of nanostructures by femtosecond laser for surface-enhanced Raman scattering," Opt. Express **17**(24), 21581–21589 (2009).
7. K. D. Alexander, M. J. Hampton, S. Zhang, A. Dhawan, H. Xuc, and R. Lopeza, "A high-throughput method for controlled hot-spot fabrication in SERS-active gold nanoparticle dimer arrays," J. Raman Spectrosc. **40**(12), 2171–2175 (2009).
8. I. M. White, J. Gohring, and X. Fan, "SERS-based detection in an optofluidic ring resonator platform," Opt. Express **15**(25), 17433–17442 (2007).
9. S. Kim, W. Zhang, and B. T. Cunningham, "Photonic crystals with SiO_2-Ag "post-cap" nanostructure coatings for surface enhanced Raman spectroscopy," Appl. Phys. Lett. **93**(14), 143112 (2008).

#121459 - $15.00 USD Received 8 Jan 2010; revised 4 Feb 2010; accepted 11 Feb 2010; published 17 Feb 2010

10. W. Zhang, N. Ganesh, I. D. Block, and B. T. Cunningham, "High sensitivity photonic crystal biosensor incorporating nanorod structures for enhanced surface area," Sens, Actuator B-Chem. **131**(1), 279–284 (2008).
11. W. Zhang, N. Ganesh, P. C. Mathias, and B. T. Cunningham, "Enhanced fluorescence on a photonic crystal surface incorporating nanorod structures," Small **4**(12), 2199–2203 (2008).
12. W. Zhang, and B. T. Cunningham, "Fluorescence enhancement by a photonic crystal with a nanorod-structured high index layer," Appl. Phys. Lett. **93**(13), 133115 (2008).
13. S. M. Kim, H. Kim, and S. Kang, "Development of an ultraviolet imprinting process for integrating a microlens array onto an image sensor," Opt. Lett. **31**(18), 2710–2712 (2006).
14. C. Oubre, and P. Nordlander, "Finite-difference time-domain studies of the optical properties of nanoshell dimers," J. Phys. Chem. B **109**(20), 10042–10051 (2005).
15. S. B. Chaney, S. Shanmukh, R. A. Dluhy, and Y.-P. Zhao, "Aligned silver nanorod arrays produce high sensitivity surface-enhanced Raman spectroscopy substrates," Appl. Phys. Lett. **87**(3), 031908 (2005).
16. N. M. B. Perney, J. J. Baumberg, M. E. Zoorob, M. D. B. Charlton, S. Mahnkopf, and C. M. Netti, "Tuning localized plasmons in nanostructured substrates for surface-enhanced Raman scattering," Opt. Express **14**(2), 847–857 (2006).
17. http://www.d3diagnostics.com/en/klarite-substrates–10452

1. Introduction

Surface enhanced Raman spectroscopy (SERS) is one of the most sensitive techniques available for providing specific chemical identification, and has generated tremendous interest in the field of biomolecule detection [1]. The mechanisms of SERS are currently a subject of debate, and two main enhancement routes have been proposed – namely the electromagnetic (EM) effect [2] and the chemical enhancement effect [3]. For the EM effect, the local EM field at the surface of a metal is significantly different from that of the incident field, and that difference becomes more pronounced when fine metal particles or rough surfaces generate local surface plasmon resonance (SPR). Various metal nanostructures have been proposed to obtain high SERS enhancement factor (EF) and SERS EF of 10^6~10^9 were demonstrated in previous research [4–7]. However, additional enhancement of SERS signals is still required for detecting trace quantities of drugs-of-abuse, biological pathogens and environmental contaminants. To obtain the additional SERS EF to the metal nanostructure, metal-dielectric optical resonators have been proposed which can couple SPR effects of metal nanostructures with the resonance effects of dielectric optical resonators. For example, Fan, et. al. [8] suggested a liquid core optical ring resonator that can couple the enhanced EM fields of a ring resonator to the EM fields generated by metal nanoparticles which pass through the channel with target analytes to obtain a higher Raman signal. Previously, we have proposed and demonstrated a photonic crystal (PC) surface dielectric resonator with SiO_2–Ag "post-cap" nanostructure coatings as a SERS substrate (PC-SERS), which can provide additional SERS EFs using the enhanced near-field generated by the PC [9].

Metal-dielectric optical resonators are attractive in the fields of biomolecular sensing and industrial process monitoring applications, because the higher enhanced EM fields from the dielectric resonator can increase the energy available for surface plasmons, thereby increasing detection sensitivity. However, one critical factor that must be considered in the design of a metal-dielectric optical resonator is that a balance must be achieved between locating the metal nanostructures too close to the dielectric resonator surface while locating them within the evanescent field of the dielectric resonator to achieve sufficient surface plasmon coupling efficiency, because metal absorption will deteriorate the resonance characteristics of the dielectric resonator. Meanwhile, the intensity of the resonant EM field of the dielectric resonator decays exponentially with distance from the dielectric resonator surface, thus resulting in a tradeoff for obtaining the optimal metal volume density and spatial distribution. In this study, to maximize the additional SERS EF due to the dielectric optical resonator, the effects of the distance between the dielectric optical resonator and the metal nanoparticles as well as the size of the metal nanoparticles on the coupling efficiency were examined using simulation and experimental methods with our PC-SERS substrate structure, which provide a large-area platform that can be used to uniformly provide an increased surface-bound electric field for exciting surface plasmons in metal nanoparticles. The far-field and near-field

#121459 - $15.00 USD Received 8 Jan 2010; revised 4 Feb 2010; accepted 11 Feb 2010; published 17 Feb 2010

characteristics of the PC-SERS substrate were analyzed by measuring the transmission spectrum and by simulating the enhanced near-electromagnetic fields using rigorous coupled wave analysis (RCWA) while varying the SiO_2 "post" layer and Ag "cap" layer thicknesses to examine the coupling efficiency. The SERS EF of the PC-SERS substrate given various design configurations were also analyzed by measuring the Raman signal of trans-1,2-bis(4pyridyl)ethane on the PC-SERS substrates. The effectiveness and limitation of the proposed PC-enhancement platform were discussed by comparing the Raman signal form PC-SERS and commercially available SERS substrates.

2. Fabrication of PC-SERS substrates

Figure 1(a) shows three-dimensional schematic model of the PC-SERS substrate, which is comprised of a 1-dimensional (1-D) PC slab and a SiO_2-Ag "post-cap" nanostructure coating, where t_p is the SiO_2 "post" thickness and t_c is the Ag "cap" thickness. The PC is a periodic arrangement of dielectric materials with sub-wavelength pitch, and the period, grating depth, film thicknesses, and the refractive indexes of its materials are chosen in such a way that the PCs can support guided-mode resonances (GMR), where the device reflects ~100% of the incident light at the resonant wavelengths while all other wavelengths are transmitted. Under resonant conditions, excited leaky modes are localized in space during their finite lifetimes, which enhances the near EM-field intensity of the PC structure [10–12]. The enhanced near-EM fields of a PC can efficiently couple light from a laser to the metal nanostructures on the PC-SERS surface, and can increase the EM-field intensity around the metal. The 1-D PC slab was fabricated using nanoreplica molding technique [13] to produce the grating structure and physical deposition processes to provide the dielectric thin films. Nanoreplica molding using UV-curable polymers is the primary fabrication technique for the grating due to its ability to produce nanostructures inexpensively and with the repeatability and uniformity required for a reliable biosensor. A silicon wafer is used as a mold by fabrication of a negative volume image of the desired surface structure patterned using reactive ion etching through a mask produced by deep-UV photolithography (grating period = 360nm, duty cycle = 50% and depth = 60nm). After stripping away the photoresist, the silicon mold wafer was treated with a self assembled monolayer (SAM) silane coating to prevent adhesion of cured polymer to the wafer. The SAM film was applied by dipping the wafer into a 2% solution of dimethyldichlorosilane dissolved in octamethylcyclooctasilane. A UV-curable epoxy liquid was dispensed onto the silicon wafer in several small droplets, and squeezed into a uniform thin film between the silicon and a flexible sheet of polyester substrate. A high intensity UV lamp illuminates epoxy though the polyester substrate to cure the replication material, minimizing thermal defects. After the curing process, the replicated grating structure and silicon master were separated. Dielectric films of SiO_2 with a thickness of ~300nm (n = 1.46) and TiO_2 with a thickness of ~100 nm (n = 2.25) were deposited over the replicated grating structure to fabricate the PC structure. The thick SiO_2 layer is designed to physically separate the resonant near fields from the polymer to reduce the undesired background fluorescence from the polymer [11].

The oblique angle deposition (OAD) method was used to fabricate the SiO_2–Ag "post-cap" nanostructure on the PC slab. OAD uses a conventional e-beam evaporator that typically provides solid think films, but with a substrate holder that enables the angle between the evaporating flux and the surface of the substrate is less than 15° [10–12]. When the mobility of atoms is limited, a self-shadowing effect during deposition results in a highly porous film with a structure composed of isolated vertical nanorods. The OAD is advantageous for producing a high density layer of nanostructures because it does not require lithography, and be performed with a high degree of uniformity over large surface areas. Any material that can be evaporated can be applied by the OAD method, and using a system that contains more than one evaporant source, it is possible to alternate between materials to form composite nanostructures. Incorporation of substrate rotation into an OAD system (glancing angle

#121459 - $15.00 USD Received 8 Jan 2010; revised 4 Feb 2010; accepted 11 Feb 2010; published 17 Feb 2010

deposition, GLAD) enables formation of straight nanorods or helical nanorods, but in the work reported here, no substrate rotation was used, resulting in nanorods that lean towards the evaporant source by ~55 °. An electron-beam deposition system with a deposition rate of 5 Å/s and an incoming flux angle of 5 ° was used for the OAD coating of SiO_2 and Ag on the PC substrate. Figure 1(b) shows the cross sectional scanning electron microscope (SEM) image of a typical SiO_2-Ag "post-cap" nanostructure (t_p = 75 nm, t_c = 20 nm), which was fabricated on the silicon substrate for the SEM measurement. For comparison, the same SiO_2-Ag "post-cap" nanostructures were also fabricated on an ordinary glass slide (GL-SERS).

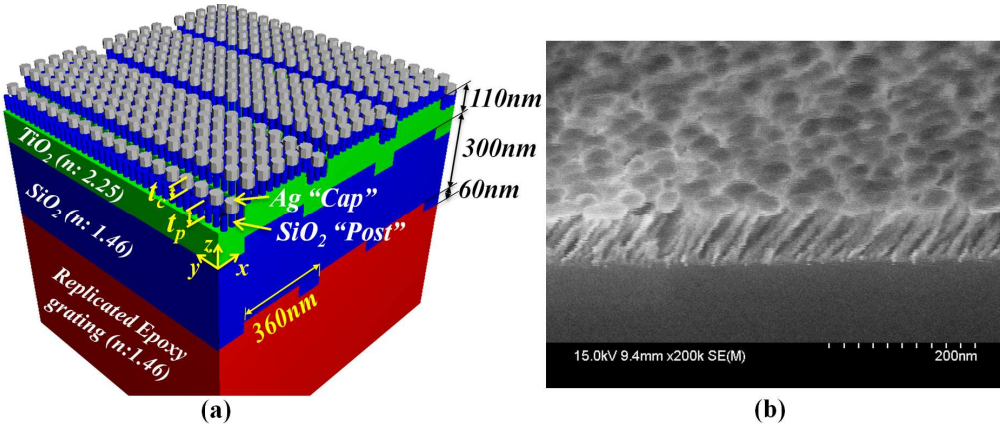

Fig. 1. (a) Schematic diagram of PC-SERS substrate and (b) cross sectional SEM image of SiO_2-Ag "post-cap" nanostructure with a thickness of SiO_2 layer of 75nm and a thickness of Ag layer of 20nm by OAD method.

3. Far-field characteristics of PC-SERS substrates

To examine the coupling efficiency of a PC surface to a layer of discrete metal nanoparticles applied to the PC surface by the OAD method, the far-field characteristics of the PC-SERS substrate were assessed. We compared the transmission efficiency as a function of wavelength for a PC without a post-cap coating to a PC-SERS substrate and a GL-SERS substrate. The transmission spectra of the fabricated bare PC substrate, GL-SERS substrate, and PC-SERS substrate with different SiO_2 "post" layer thicknesses were measured and compared as depicted in Fig. 2. The fabricated PC substrate has a resonant transmission peak for the TE polarized (electric field parallel to the grating lines) light with a wavelength of 630nm at normal incidence, and also has a resonance reflection for the laser used to excite SERS (λ = 600 nm, TE polarized) at an incident angle of ~13 °, as shown in Fig. 2(a). Figures 2(b) and 2(c) show the measured transmission spectra of a GL-SERS substrate and a PC-SERS substrate and the expected spectra of PC-SERS, which was calculated using the product of the measured transmission of the bare PC substrate and the GL-SERS substrate, for the different SiO_2-Ag "post-cap" nanostructures, (b) t_p = 0 nm, t_c = 40 nm, and (c) t_p = 50 nm, t_c = 40 nm. The data clearly shows that the SiO_2 "post" layer can prevent quenching of resonant near-fields of the PC due to the closely located high-loss metal structure and the quality factor of the PC resonance (Q, ratio of the full width at half maximum (FWHM) of the resonance peak to the peak wavelength) reduces from Q = 18.75 to Q = 10 as the SiO_2 "post" height decreases from t_p = 50 to t_p = 0 nm.

#121459 - $15.00 USD Received 8 Jan 2010; revised 4 Feb 2010; accepted 11 Feb 2010; published 17 Feb 2010

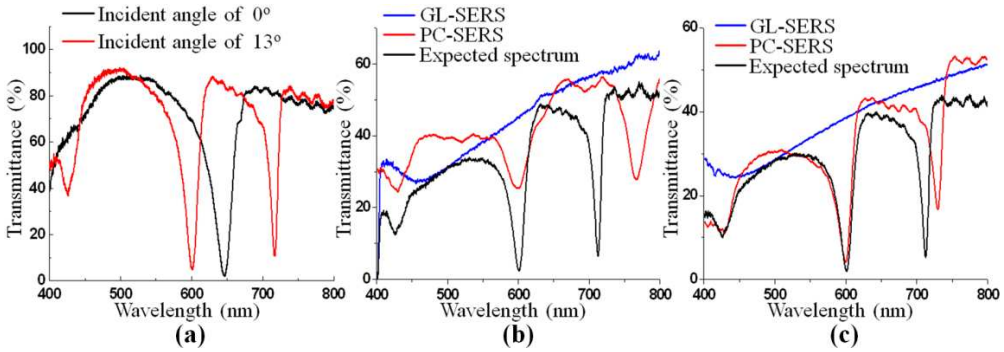

Fig. 2. Comparison of measured transmission spectra (a) from bare PC at the incident angles of 0° and 13° and from GL-SERS and PC-SERS substrate (b) with Ag nanostructures without SiO_2 "post" (t_p = 0 nm, t_c = 40 nm), and (c) with 50 nm SiO_2 "post" and 40nm Ag "cap" (t_p = 50 nm, t_c = 40 nm) at the incident angle of 13°; The expected spectrum in (b) and (c) were calculated spectrum from measured transmission of GL-SERS and bare PC substrates.

4. Simulation and experimental methods to examine coupling efficiency

To examine the coupling effects of the enhanced EM fields due to metal nanostructure and PC in detail, the near-field characteristics of PC-SERS substrate were examined by simulation and experiment. An RCWA software package (Diffract MOD, RSOFT, USA) was used to calculate the EM amplitude distribution around a single Ag nanostructure on the PC-SERS and GL-SERS substrates. Since the SiO_2–Ag "post-cap" nanostructure fabricated using the OAD technique is a randomly distributed and sized structure, exact modeling of the nanostructured coating would require greater computational resources than are readily available, so a simplified structure was considered instead as a means of visualizing the electric field surrounding the Ag nanoparticles. For the SiO_2 nanopost layer, a uniform layer comprised of a 65:35 mixture of air:SiO_2 was used for the simulation, as described in our previous work using OAD-deposited dielectric nanostructures [12,13]. For the Ag nanostructure, a cylindrical Ag metal nanoparticle with a diameter of 40 nm, designed height, and pitch of 60 nm was used for the simulation model, because the measured diameters of the Ag nanostructures from SEM images were 30 ~50 nm, and the simulated transmission spectra using these dimensions were similar to the transmission spectra measured from the GL-SERS substrates. Although this model cannot exactly predict the characteristics of real SiO_2–Ag "post-cap" nanostructures, we believe that this model can demonstrate the effect of GMR from the PC upon the EM-field distribution around Ag nanoparticles above the PC surface. Figure 3 shows the simulated x-y plane EM amplitude distribution for a single Ag nanostructure (a) on a GL-SERS substrate, (b) on a PC-SERS substrate at off-resonance condition and (c) on a PC-SERS substrate at on resonance condition, which have the same SiO_2-Ag "post-cap" nanostructure (t_p: 50 nm, t_c: 40nm) and illuminated with a TE polarized plane wave source (λ = 600 nm, incident E field magnitude = 1 V/m). An enhanced EM field is generated around the Ag nano particles due to the SPR effect of the metal structure, and the maximum EM field amplitude is increased from 47.88 to 110.42 V/m due to the GMR effect of the PC. Since the Raman signal is proportional to the 4th power of the electric field amplitude ($|E|^4$) [14], we calculate that the $|E|^4$ distribution around the Ag nanostructure, and the average value of $|E|^4$ in the volume surrounding the metal particle was defined as the EM field intensity (*EMI*) for comparison. The *EMI* for GL-SERS and PC-SERS at resonance were defined as EMI_{NANO} and EMI_{TOT}, and the *EMI* enhancement due to the PC was defined as EMI_{PC}, which is the ratio of EMI_{TOT} to EMI_{NANO}. The EMI_{NANO} and EMI_{TOT} calculated in Fig. 3 were 1081.7 and 16929, respectively, and the EMI_{PC} was 15.56.

To experimentally examine the coupling effects of the enhanced EM fields, the SERS enhancement factor was measured. A Raman spectrum of trans-1,2-bis(4pyridyl)ethane (BPE)

#121459 - $15.00 USD Received 8 Jan 2010; revised 4 Feb 2010; accepted 11 Feb 2010; published 17 Feb 2010

on the PC-SERS substrate was measured and compared with those on a GL-SERS substrate and in a liquid high concentration droplet. A Raman detection instrument comprised of a TE polarized excitation source (λ = 600 nm, Output power = 82 mW), a sample holder with a rotational stage, a power meter to measure laser transmittance through the sample, and a spectrometer was used for the measurement as depicted in Fig. 4(a). The diameter of the laser beam spot was ~470 μm, and Raman scattered light was collected from a 235.4 × 51.8 μm^2 area. A 5 μL droplet of BPE dissolved in methanol (6.36×10^{-3} M) was applied to each substrate using a pipette. The BPE/methanol droplet spread out to form a circular region with a diameter of ~1.6 cm on the substrate, resulting in a density of ~9.5×10^{15} molecules/cm^2. For a laser wavelength of 600 nm, the PC resonance could be excited by illuminating at an angle of ~ ± 13 °, and precise tuning to the "on-resonance" condition for any substrate could be achieved by adjusting the rotation stage to obtain a minima in the laser transmitted intensity through the PC. "Off-resonance" conditions were obtained by detuning the incident angle from the transmission minima by ~ ± 13 °. Figure 4(b) shows the measured Raman spectrum obtained from the BPE on GL-SERS substrate with a thickness of Ag "cap" layer of 40nm. The Raman peaks at 1000, 1200, 1610 and 1639 cm^{-1} can be found and these peaks correspond to the ring-breathing mode of pyridine, the C = C stretching mode, the aromatic ring stretching mode, and the in-plane ring mode, respectively [9]. To define the SERS EF, the Raman signal was defined as the integrated intensity of the 1200 cm^{-1} peak after subtraction of the background noise and the Raman signal in Fig. 4(b) was 20465.

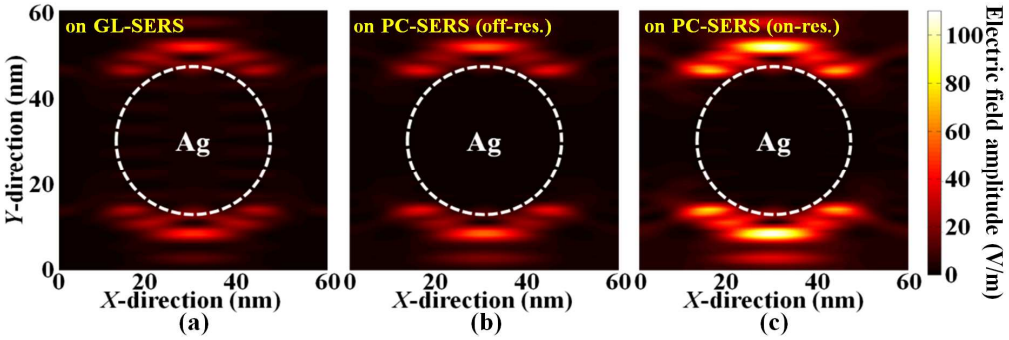

Fig. 3. Simulated x-y plane EM amplitude distribution (z: top of Ag nanorods) for a single Ag nanostructure (a) on a GL-SERS substrate and (b), (c) on a PC-SERS substrate, which have the same SiO_2-Ag "post-cap" nanostructure (t_p: 50 nm, t_c: 40nm) and illuminated with a TE polarized plane wave source (λ = 600 nm, incident E field magnitude = 1 V/m) at (a), (b) normal incident and (c) at a incident angle of ~13° (on-resonance condition)

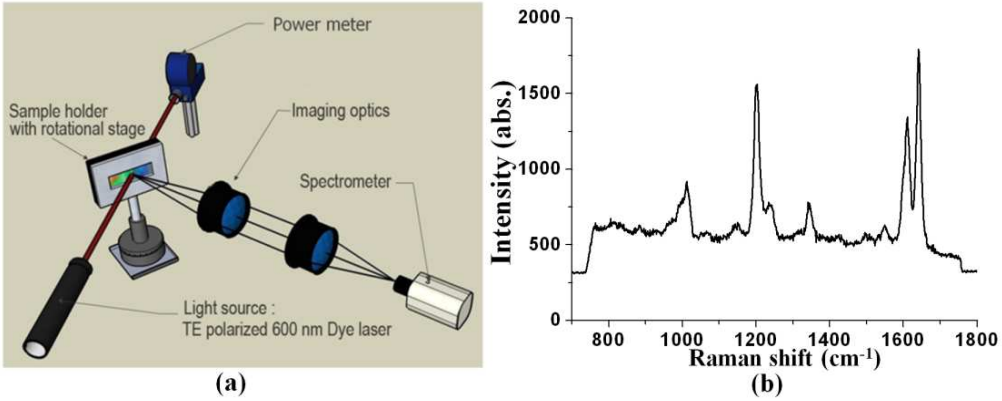

Fig. 4. (a) Schematics of the Raman detection instrument for PC-SERS and (b) measured Raman spectrum of BPE on GL-SERS substrate (t_p = 0 nm, t_c = 40 nm).

#121459 - $15.00 USD Received 8 Jan 2010; revised 4 Feb 2010; accepted 11 Feb 2010; published 17 Feb 2010

The SERS EF is defined as $EF = (I_{SERS} / t_{SERS} N_{SERS})(I_{Ref} / t_{Ref} N_{Ref})^{-1}$, where I_{SERS} and I_{Ref} are the Raman signals from the SERS substrate and a reference substrate, respectively. t is the detection integration time for each measurement, and the N is the number of excited molecules. To establish a baseline from which the EF attributable to either the PC or the SiO_2-Ag nanostructure could be calculated, two references are required. For a baseline reference, the Raman signal from a droplet of BPE in methanol at a high concentration (0.636 M) on a plain glass surface was used, denoted by I_0. A second reference, denoted by I_{Nano}, was obtained by measuring the SERS signal on a GL-SERS substrate with a 100x lower BPE concentration. The EF attributed only to the "post-cap" nanostructure coating is therefore $EF_{NANO} = 100(I_{NANO} t_0) / (I_0 t_{NANO})$. The Raman signal of the PC-SERS substrate, obtained from the Raman spectrum at the on-resonance condition using 0.00636 M BPE, is denoted by $I_{PC\text{-}SERS}$. The overall EF, using both effects together, is $EF_{TOT} = 100(I_{PC-SERS} t_0) / (I_0 t_{PC-SERS})$ and the EF due to the PC is given by $EF_{PC} = (I_{PC-SERS} t_{NANO}) / (I_{NANO} t_{PC-SERS}) = EF_{TOT} / EF_{NANO}$. For these experiments t_0 = 600 sec, t_{Nano} = 50 sec, and $t_{PC\text{-}SERS}$ = 50 sec.

5. Effects of SiO_2 –Ag "post-cap" thicknesses on the coupled EM fields and SERS EF

To examine the effects of the Ag "cap" and the SiO_2 "post" layer thicknesses on the *EMI* and SERS EF, PC-SERS and GL-SERS substrates with an Ag "cap" layer thickness ranging from 20 to 60 nm and a SiO_2 "post" layer thickness ranging from 0 to 75 nm were designed and fabricated. Two 1x3 $in.^2$ (1 in. = 2.54 cm) samples (same as conventional glass microscope slide) were fabricated for each structural design and more than five Raman signals were obtained for each sample to calculate SERS EF. Figure 5 shows the effects of the SiO_2 "post" thickness on (a) simulated EMI_{NANO}, EMI_{TOT}, and EMI_{PC}, and (b) measured EF_{NANO} and EF_{TOT} (mean value and standard deviation), and EF_{PC} (calculated using mean values) for a fixed Ag "cap" thickness of 40 nm and variable SiO_2 "post" heights.

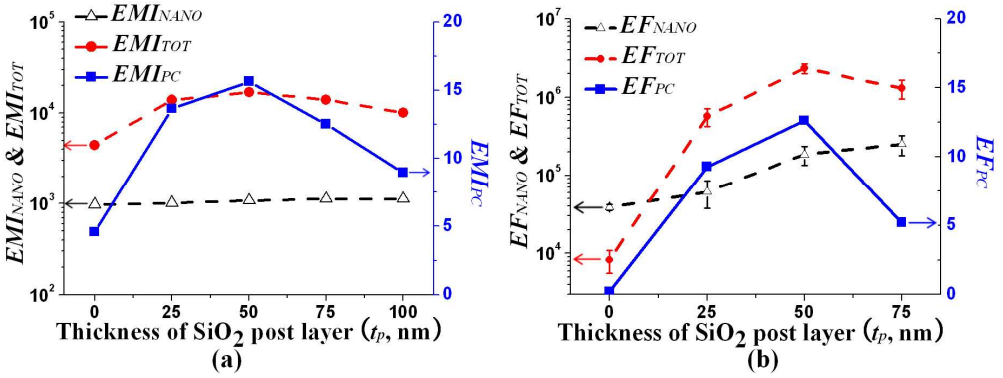

Fig. 5. Effects on (a) simulated EMI_{NANO}, EMI_{TOT} and EMI_{PC}, and (b) measured EF_{NANO}, EF_{TOT}, and EF_{PC} at varying SiO_2 "post" layer thicknesses for a fixed Ag "cap" thickness of 40nm.

Figure 5(a) shows that the EMI_{NANO} is almost independent of the SiO_2 "post" thickness. However, the EMI_{TOT} and EMI_{PC} are increased up to a SiO_2 "post" height of 50 nm, because the GMR of PC degrades as the metal becomes too close to the PC surface. The EMI_{TOT} for a 75 and 100 nm SiO_2 "post" is lower than that at 50 nm, because the intensity of the resonant near-field of the PC decays exponentially with distance from the PC surface. In Fig. 5(b), the maximum EF_{PC} is obtained with a SiO_2 "post" height of 50 nm, just as for the EMI_{PC}, but the EF_{NANO} increased with the increasing thickness of the SiO_2 "post". Since the EF_{NANO} is affected only by the Ag nanostructure, it shows that the shapes of the OAD Ag nanorods are affected by the thickness of the SiO_2 "post". When Ag was deposited on the SiO_2 "post" layer, some Ag particles might insert into the gaps between SiO_2 "post", so that the Ag "cap"

#121459 - $15.00 USD Received 8 Jan 2010; revised 4 Feb 2010; accepted 11 Feb 2010; published 17 Feb 2010

nanostructure on a thicker SiO_2 "post" layer might have a higher aspect ratio. The higher aspect ratio of the Ag nanostructure can generate the higher enhanced EM field due to the SPR which increase the SERS EF (electromagnetic effects) [15], and also provide higher surface area, which increase the number of molecules absorbed on the metal nanostructure and SERS EF (chemical effects). The coefficient of variation (%CV) of measured SERS EF (3-30%) was relatively large because the BPE molecules on the SERS substrate were not uniformly distributed after drying of deposited droplets. Figure 6 shows the effects of the Ag "cap" thickness on the measured EF_{NANO}, EF_{TOT}, and EF_{PC} for a fixed SiO_2 "post" thickness of 50 nm and variable Ag "cap" height. By increasing the thickness of the Ag "cap" layer, the EF_{NANO} is increased because the high aspect ratio Ag nanostructure can generate a higher EM field and provide a higher surface area. However, thicker Ag nanorods prevent light from reaching the PC surface from the excitation source, resulting in a reduced resonant EM near-field on the PC surface. Thus, the EF_{PC} decreases as the Ag thickness increases. Experimentally, we observe that EF_{PC} decreased from 21.4 × to 7.8 × as the Ag "cap" thickness increased from 20 to 60 nm. From these simulation and experiment methods, the optimal nanostructure was selected to have an Ag thickness of 40nm and an SiO_2 thickness of 50nm to maximize the SERS EF of the PC-SERS substrate, in which we obtain a 2.34×10^6 SERS EF including an enhancement factor of 12.6 × due to the PC structure. Figure 7 shows the comparison of measured Raman spectra obtained from the BPE on both GL-SERS and PC-SERS substrates at on- and off-resonance conditions (t_p: 50 nm, t_c: 40nm). The Raman signal for GL-SERS, PC-SERS at off- resonance and PC-SERS at resonance were 83522, 202780, and 1168800, respectively. The Raman signal from the PC-SERS substrate at off-resonance condition was 2.4 times larger than that from GL-SERS substrate, and that from PC-SERS substrate at on-resonance condition was 14 times larger than that from GL-SERS substrate for this typical example. It clearly shows the Raman signal enhancement due to the GMR effect of the PC.

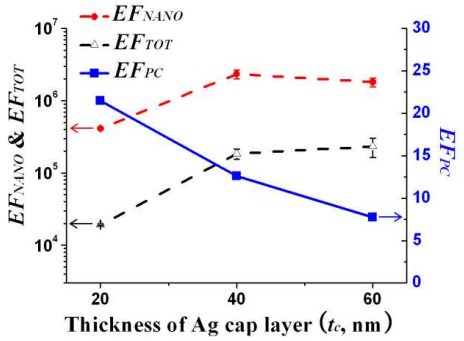

Fig. 6. Effects on the measured EF_{NANO}, EF_{TOT}, and EF_{PC} varying thickness of Ag "cap" layer for a fixed SiO_2 "post" thickness of 50nm.

#121459 - $15.00 USD Received 8 Jan 2010; revised 4 Feb 2010; accepted 11 Feb 2010; published 17 Feb 2010

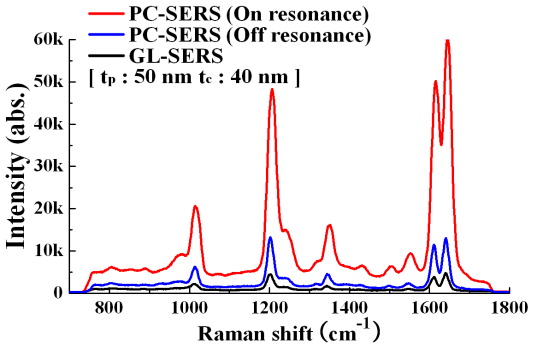

Fig. 7. Comparison of measured Raman spectra of BPE on GL-SERS and PC-SERS substrate (on and off resonance condition) with a SiO_2 "post" thickness of 50nm and Ag "cap" height of 40nm.

6. Discussion

The goal of the PC-enhancement is to provide a large-area platform that can be used to uniformly provide an increased surface-bound electric field for exciting surface plasmons in metal nanoparticles. Although the measured SERS EF at the optimal PC-SERS structure by our calculation (2.34×10^6) was relatively lower than that obtained in recent papers [4–7], there are still several aspects that are not optimized. For example, by matching the resonance wavelengths the SPR of the nanostructure to the GMR of the PC, we would expect to obtain a greater electromagnetic enhancement, especially for illumination of the structure through the PC substrate. The PC surface could be used to enhance other SERS-active surfaces besides the post-cap structure presented in this work. For example, silver nano particle surfaces generated by femtosecond laser ablation [6], which have demonstrated enhancement factors of up to 10^9 without the use of a PC surface, would be compatible with the approach described here. Since there is an assumption of counting the number of molecules excited in the calculation of SERS EF, we also undertook an experiment to compare SERS signals for BPE deposited on the PC-SERS substrate and a commercially available SERS substrate (Klarite® 302, D3 Technologies Ltd., UK) [16,17] with identical BPE concentration and measurement conditions to estimate the SERS EF of the PC-SERS. The Klarite® SERS substrate is comprised of an array of inverse pyramids etched into a silicon substrate with a period of 2 μm and depths of 0.7 μm to 1.0 μm. The silicon surface structure of the Klarite® substrate is overcoated with a 300nm layer of Au, and has a reported enhancement factor of 10^6. Figure 8 shows the measured Raman spectra obtained from BPE on the Klarite® SERS substrate and PC-SERS substrate with 50 nm SiO_2 "post" layer and 40 nm Ag "cap" layer. A 2 μL droplet of BPE dissolved in methanol (6.36×10^{-3} M) was applied to each substrate using a pipette, and the accumulation time of 50 s and output power of Laser of 54mW were used for this measurement. The Raman signal (mean) for the 1200^{-1} Raman peak for PC-SERS was 148,070 and that for Klarite® SERS substrate was 3,719. It is noted that the PC-SERS device with 50nm SiO_2 "post" layer and 40nm Ag "cap" layer demonstrates a ~40 x increased Raman signal, thus we can estimate an enhancement factor of ~4.0 x 10^7 for the structure reported here. While this enhancement is not greater than several recent reports of enhancement factors exceeding 10^8 [5–7], the enhancement was obtained on a surface that has a dense population of metal nanoparticles, providing an opportunity for a greater number of molecules to encounter a hot spot than methods with a surface only sparsely populated with hot spots. Further, the BPE molecule detection shown here does not form a self-assembled monolayer with Ag, which can further reduce the maximum enhancement factor.

#121459 - $15.00 USD Received 8 Jan 2010; revised 4 Feb 2010; accepted 11 Feb 2010; published 17 Feb 2010

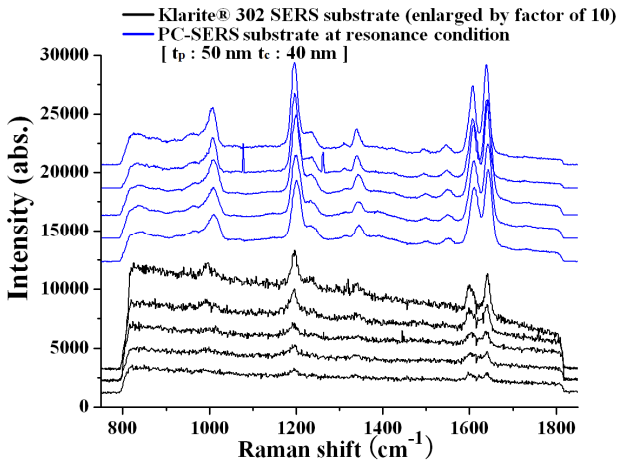

Fig. 8. Comparison of Raman spectra of BPE on Klarite® SERS substrate and PC-SERS substrate at resonance condition; the spectra for Klarite® SERS substrate was enlarged by a factor of 10.

7. Conclusions

In conclusion, we have presented the effects of the structural parameters of the SiO_2-Ag "post-cap" nanostructures on the measured transmission spectrum, simulated EM field around the Ag nanoparticles, and the measured SERS signal of BPE on the PC-SERS substrate to maximize the additional EF due to the GMR of the PC. Both the simulation and experiment results show that the coupling efficiency of the SPR effect and the GMR effect are affected by the structural parameters of the SiO_2-Ag "post-cap" nanostructures, and an optimization is required to obtain maximum coupling efficiency. Our results show that SiO_2 "posts" that are too short can diminish the resonance characteristics of PC when the metal nanoparticles are extremely close to the PC surface, while SiO_2 "posts" that are too tall will decrease the coupling efficiency due to the exponential decay of the enhanced EM field generated by the PC. Thicker Ag caps were shown to increase the SERS EF due to the SPR of the Ag nanostructure, but at the same time decreases the amount of light reaching the PC, thus reducing the PC enhancement factor when the device is illuminated from the top. In this study, using a PC-SERS substrate with 50 nm SiO_2 "posts" and 40 nm Ag "caps", resulted in a maximum SERS EF of 2.34×10^6. The SERS EF combines the effect of the SiO_2-Ag "post-cap" nanostructure with the resonant near-field of the PC, where the additional SERS EF attributable to the PC was as high as 21.4 ×. We believe that the results of this work and the supporting commentary are invaluable for the SERS substrate and for any devices which can use the coupled optical resonance effects of the metal nanostructure and dielectric optical resonator. The improvement of total SERS EF by controlling the PC structure, modifying measurement methods and applying the PC enhancement platform to alternative metallic nanostructures are the subjects of ongoing research.

Acknowledgements

This work was supported by the National Research Foundation of Korea (NRF) grant funded by the Korea Government (MEST) (No. 2009-0067065) and by SRU Biosystems.

#121459 - $15.00 USD Received 8 Jan 2010; revised 4 Feb 2010; accepted 11 Feb 2010; published 17 Feb 2010